PRAMANA — journal of physics

Vol. 78, No. 6
June 2012
pp. 927–946

Large-N_c quantum chromodynamics and harmonic sums

EDUARDO DE RAFAEL

Centre de Physique Théorique, Unité Mixte de Recherche (UMR 6207) du CNRS et des Universités Aix Marseille 1, Aix Marseille 2 et Sud Toulon-Var, affiliée à la FRUMAM, CNRS-Luminy, Case 907, F-13288 Marseille Cedex 9, France

E-mail: EdeR@cpt.univ-mrs.fr

Abstract. In the large-N_c limit of QCD, two-point functions of local operators become harmonic sums. I review some properties which follow from this fact and which are relevant for phenomenological applications. This has led us to consider a class of analytic number theory functions as toy models of large-N_c QCD which also is discussed.

Keywords. Large-N_c QCD; harmonic sums; Riemann zeros; quantum field theory.

PACS Nos 11.10.−z; 11.10.Cd; 11.10.Ef; 11.10.Gh; 11.10.Hi; 11.15.Bt; 11.55.Hx; 12.38.Cy

1. Introduction

Many of us would like to know the answer to the following questions:

- What is the effective field theory of QCD at long distances?
- How does QCD fix the couplings of the chiral Lagrangian of the Nambu–Goldstone modes of the spontaneously broken chiral-$SU(3)$ flavour symmetry?
- Can we answer these questions, perhaps more easily, within the framework of QCD in the large-N_c limit [1]?

  In that respect, it has been shown (see refs [2–5]. For a lucid exposition, see ref. [6]) that if the confinement property of QCD persists in this limit there is also spontaneous chiral symmetry breaking and the hadronic spectrum consists then of an infinite number of narrow states [7].

Unfortunately, in spite of the successes of the Standard Model, the answer to these questions remains unknown. What I shall do here is to provide a few comments related to them.

1.1 *General comments*

(1) Independently of the large-N_c approximation, the couplings of the effective chiral Lagrangian of the strong interactions of the Nambu–Goldstone modes can be

DOI: 10.1007/s12043-012-0319-0; ***e*Publication: 8 June 2012**

identified with the coefficients of the Taylor expansion of appropriate QCD Green's functions.

(2) By contrast, most of the couplings of the effective chiral Lagrangian of the electroweak interactions of the same Nambu–Goldstone modes are given by integrals over all the ranges of Euclidean momenta of appropriate two-point functions with soft insertions of local operators. Their determination, therefore, requires a precise matching of the short-distance and the long-distance contributions to the underlying QCD Green's functions.

Typical terms of the chiral Lagrangian are:

$$\mathcal{L}_{\rm eff} = \frac{1}{4}F_\pi^2 \underbrace{{\rm tr}(D_\mu U D^\mu U^\dagger)}_{\pi\pi\to\pi\pi\,,\ K\to\pi e\nu} + \mathcal{L}_{WZW} + \underbrace{L_{10}\,{\rm tr}(U^\dagger F_{R\mu\nu} U F_L^{\mu\nu})}_{\pi\to e\nu\gamma} + \cdots$$

$$\underbrace{e^2 C\,{\rm tr}(Q_R U Q_L U^\dagger)}_{-e^2 C\frac{2}{F_\pi^2}(\pi^+\pi^- + K^+K^-)} - \underbrace{\frac{G_{\rm F}}{\sqrt{2}} V_{ud}V_{us}^*\, g_{\underline{8}}\, F_\pi^4 \left(D_\mu U D^\mu U^\dagger\right)_{23}}_{K\to\pi\pi,\ K\to\pi\pi\pi} + \cdots . \quad (1.1)$$

Here U denotes the 3×3 unitary matrix in the u, d, s flavour space which collects the Nambu–Goldstone fields and which under chiral rotations transforms as $U \to V_{\rm R} U V_{\rm L}^\dagger$; $D_\mu U$ denotes the covariant derivative in the presence of external vector and axial-vector sources. The first term in the first line is the lowest-order effective Lagrangian in the sector of the strong interactions [8] with F_π the pion-decay coupling constant in the chiral limit where the light quark masses u, d, s are neglected ($F_\pi \simeq 90$ MeV). The second term stands for the anomalous Wess–Zumino–Witten [9,10] effective Lagrangian of $\mathcal{O}(p^4)$. The third one shows a typical term of $\mathcal{O}(p^4)$ in the chiral counting [11], with L_{10} a coupling constant which is not fixed by symmetry requirements alone. The first term in the second line corresponds to the lowest-order effective Lagrangian, which is $[\mathcal{O}(p^0)]$ in the chiral counting [12], and which appears when photons are integrated out in the presence of strong interactions ($Q_{\rm L} = Q_{\rm R} = {\rm diag.}[2/3, -1/3, -1/3]$ and e is the electric charge). The second term in the second line is the lowest-order effective Lagrangian in the electroweak sector which induces non-leptonic K-decays ($G_{\rm F}$ is the Fermi constant and V_{ud}, V_{us}^* are the matrix elements of the flavour mixing matrix. The coupling $g_{\underline{8}}$ governs the strength of the dominant $\Delta I = 1/2$ transitions (for more details, see ref. [13] and references therein)). Typical physical processes to which each term contributes are indicated under the braces. Each term in the chiral Lagrangian is modulated by a coupling constant ($F_\pi^2\,, L_{10}\,, \ldots C, g_{\underline{8}} \cdots$ in eq. (1.1)), which encodes the underlying dynamics responsible for the appearance of the corresponding effective term. The evaluation of these couplings from the underlying QCD Lagrangian is the question we are interested in.

1.2 *The left–right correlation function*

As a precise example of the comments in the previous subsection, let us consider the left–right correlation function:

$$\Pi_{\rm LR}^{\mu\nu}(q) = 2i \int {\rm d}^4x\, {\rm e}^{iq\cdot x} \langle 0\,|\,T(L^\mu(x) R^\nu(0)^\dagger)\,|\,0\rangle\,, \quad (1.2)$$

with left and right currents:

$$L^\mu(x) = \bar{d}(x)\gamma^\mu \frac{1}{2}(1-\gamma_5)u(x) \quad \text{and} \quad R^\mu(x) = \bar{d}(x)\gamma^\mu \frac{1}{2}(1+\gamma_5)u(x). \tag{1.3}$$

The discussion here, unless explicitly mentioned, does not use the large-N_c approximation. In the chiral limit where the light quark masses are set to zero, this two-point function only depends on one invariant function ($Q^2 = -q^2 \geq 0$ for q^2 space-like)

$$\Pi^{\mu\nu}_{\rm LR}(q) = (q^\mu q^\nu - g^{\mu\nu}q^2)\Pi_{\rm LR}(Q^2). \tag{1.4}$$

The self-energy function $\Pi_{\rm LR}(Q^2)$ in the chiral limit vanishes order by order in QCD perturbation theory and is an order parameter of the spontaneous breakdown of chiral symmetry for all values of the momentum transfer [14]. In what follows we shall be working in this limit.

The Taylor expansion of $\Pi_{\rm LR}(Q^2)$ at low Q^2 is a power series in Q^2:

$$-Q^2\Pi_{\rm LR}(Q^2) = F_\pi^2 + 4L_{10}^{\rm eff}Q^2 + \mathcal{O}(Q^4). \tag{1.5}$$

More precisely

$$L_{10}^{\rm eff} = L_{10}(\mu) + \text{Goldstone one-loop corrections}, \tag{1.6}$$

where $L_{10}(\mu)$ denotes the $\mathcal{O}(p^4)$ coupling in eq. (1.1) renormalized at the scale μ. In the $1/N_c$ expansion, the Goldstone loop corrections are subleading and, therefore, only the tree level couplings survive in the large-N_c limit, which is one of the important simplifications of this limit.

The function $\Pi_{\rm LR}(Q^2)$ also governs the coupling constant C in eq. (1.1) and gives a mass of electromagnetic origin [15] (and also from the integration of the heavy Z electroweak boson [16]) to the $\pi^\pm$ and $K^\pm$ particles:

$$\frac{2e^2C}{F_\pi^2} = m_{\pi^\pm}^2 = m_{K^\pm}^2 = \frac{\alpha}{\pi}\frac{3}{8F_\pi^2}\int_0^\infty {\rm d}Q^2\,[-Q^2\Pi_{\rm LR}(Q^2)]. \tag{1.7}$$

This integral converges in the ultraviolet because [17]

$$\lim_{Q^2\to\infty}\Pi_{\rm LR}(Q^2) \sim \mathcal{O}\left(\frac{\langle\bar{\psi}\psi\rangle^2}{Q^6}\right). \tag{1.8}$$

Furthermore, it has also been shown [18,19] that

$$-Q^2\Pi_{\rm LR}(Q^2) \geq 0 \quad \text{for all}\, 0 \leq Q^2 \leq \infty, \tag{1.9}$$

which in particular ensures the positivity of the integral in eq. (1.7) and thus the stability of the QCD vacuum with respect to small perturbations induced by electroweak interactions.

2. Large-N_c models and phenomenology

QCD models of spontaneously chiral symmetry breaking, like the constituent chiral quark model (CχQM) of Georgi and Manohar [20–23], or the more sophisticated extended

Nambu–Jona–Lasinio (ENJL) model [24,25] have been rather successful in reproducing the phenomenological determinations of the couplings of the chiral Lagrangian in the strong interaction sector. However, they fail in general to provide the required matching between short and long distances which is needed in order to evaluate the couplings of the chiral Lagrangian induced by the electroweak interactions, i.e. couplings like C and $g_{\underline{8}}$ in eq. (1.1). Because of this, in the phenomenological applications, these models have progressively been replaced by a more direct approach where the relevant Green's functions are approximated by a finite number of the large-N_c QCD hadronic spectrum of narrow states. In fact, the resonance chiral Lagrangians of the type discussed in refs [12,26] and their extensions (see e.g. ref. [27] and references therein), can be viewed as simplified versions of the large-N_c QCD hadronic Lagrangian when limited to a finite number of states.

The methodology which has been suggested (see e.g. ref. [28] for a review), consists of fixing the couplings and masses of a minimal hadronic ansatz (MHA) of narrow states which contribute to a specific Green's function in such a way that, on the one hand the short-distance behaviour predicted by the operator product expansion (OPE) [17] of the underlying Green's function in large-N_c QCD is satisfied and, on the other hand, the long-distance behaviour constraints governed by the effective chiral Lagrangian in the sector of the strong interactions alone are satisfied as well. As an example of this MHA approach, let us consider again the integral in eq. (1.7) which fixes the coupling C. The MHA in this case requires the presence of three states: the massless pion pole, a vector state with mass M_V and an axial-vector state with mass M_A. The constraint that $\Pi_{LR}(Q^2)$ satisfies the OPE at short distances (see eq. (1.8)) implies that $\mathcal{O}(1/Q^2)$ terms and $\mathcal{O}(1/Q^4)$ terms must be absent. This, as we shall discuss later, also implies the validity of the so-called Weinberg sum rules, and fixes the couplings of the V and A states in the spectral function of the left–right correlation function with the result

$$-Q^2\Pi_{LR}(Q^2) = F_\pi^2 \frac{M_V^2 M_A^2}{(Q^2+M_V^2)(Q^2+M_A^2)}\,. \tag{2.1}$$

Inserting this function in eq. (1.7) gives a prediction for the $\pi^+ - \pi^0 \equiv \Delta m_\pi$ mass difference (this is the result for $F_\pi = (87 \pm 3.5)$ MeV, $M_V = (748 \pm 29)$ MeV and $g_A = (M_V^2/M_A^2) = 0.50 \pm 0.06$. These values follow from an overall fit to predictions of the low-energy constants in the MHA to large-N_c QCD):

$$\Delta m_\pi = (4.9 \pm 0.4)\,\text{MeV}, \tag{2.2}$$

to be compared with the experimental value: $\Delta m_\pi = (4.5936 \pm 0.0005)$ MeV.

The MHA approach to large-N_c QCD has led to a remarkable set of interesting predictions for some of the couplings of the electroweak Lagrangian in the chiral limit (two representative references are [13,29]). The incorporation of chiral corrections, however, becomes technically rather cumbersome and, above all, the question of the reliability of the approximation with a finite number of narrow states to large-N_c QCD, to which I shall later come back, remains open (see e.g. ref. [30]).

2.1 *Comment on Minkowsky vs. Euclidean*

The spectral function of the left–right correlation function defined in eq. (1.2) can be obtained from measurements of the hadronic τ-decay spectrum (vector-like decays minus

axial-vector-like decays). Figure 1 shows the experimental determination of $\frac{1}{\pi}\mathrm{Im}\Pi_{\mathrm{LR}}(t)$, obtained from the ALEPH Collaboration [31] data at LEP, vs. the invariant hadronic mass squared t in the accessible region $0 \leq t \leq m_\tau^2$. This plot is a good experimental proof of spontaneous chiral symmetry breaking in Nature. If the symmetry was realized *à la* Wigner–Weyl, the shape should be a straight horizontal line all the way down to zero. Also shown in the same figure 1 is the simple spectrum of the MHA approximation to large-N_c QCD which, as discussed before, consists of the pion pole (not shown in the figure), a vector narrow state (the first positive vertical line) and an axial-vector narrow state (the second negative vertical line). The heights of these vertical lines represent the strengths of the couplings of the narrow states in the spectral function. At this level of approximation, and in the chiral limit, the rest of the vector and axial-vector states are degenerate and, therefore, they cancel in the difference, a fact which in any case is predicted by QCD at high energies when perturbation theory applies, and is reproduced by the asymptotic horizontal continuum line shown in the figure.

Looking at the plot in figure 1, one can hardly claim that the MHA approximation in the Minkowsky region reproduces the details of the experimental data. This is to be contrasted, however, with what happens in the Euclidean region. With $\Pi_{\mathrm{LR}}(Q^2)$ determined from the spectral function by the unsubtracted dispersion relation

$$\Pi_{\mathrm{LR}}(Q^2) = \int_0^\infty \mathrm{d}t \frac{1}{t+Q^2}\frac{1}{\pi}\mathrm{Im}\Pi_{\mathrm{LR}}(t), \tag{2.3}$$

the corresponding plot of the function $(-Q^2/F_\pi^2)\Pi_{\mathrm{LR}}(Q^2)$ vs. the Euclidean variable Q^2 normalized to vector mass M_{V}^2, as shown in figure 2 (the solid curve), reproduces rather well the dotted curve, which is the one resulting from the experimental data in figure 1. This is in fact a generic feature: Green's functions in the Minkowski region have a lot of structure, while the corresponding shape in the Euclidean region shows a smooth behaviour. As shown in this example, the simple MHA in the Euclidean region already provides a rather good interpolation between the asymptotic regimes where, by

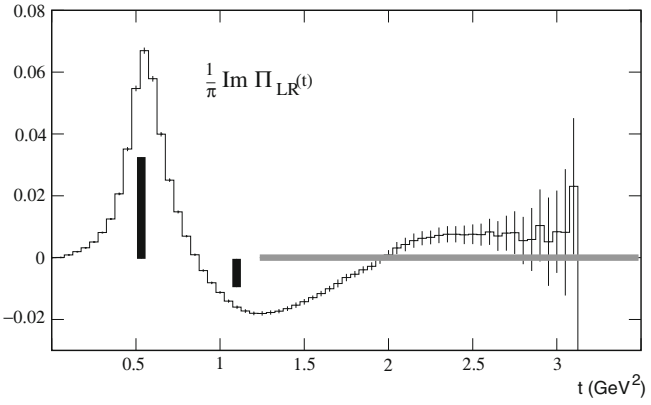

Figure 1. The spectral function $\frac{1}{\pi}\mathrm{Im}\Pi_{\mathrm{LR}}(t)$ compared to the MHA to large-N_c QCD.

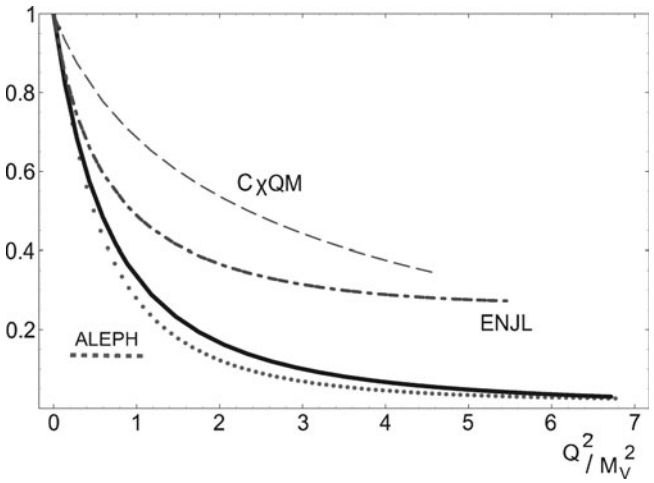

Figure 2. Plot of $(-Q^2/F_\pi^2)\Pi_{\rm LR}(Q^2)$ in the Euclidean region. The solid curve is the one corresponding to the MHA to large-N_c QCD and the dotted curve the one from the experimental data in figure 1. The other curves are the predictions of the constituent chiral quark (CχQM) model and the extended Nambu–Jona–Lasinio (ENJL) model.

construction, it has been constrained to satisfy the lowest-order chiral behaviour and the leading and next to leading OPE constraints. This good interpolation is the reason why the integral in eq. (1.7), evaluated in the MHA, already reproduces the experimental result rather well. One can also see in figure 1 that models which fail to incorporate the matching to short distances, like the CχQM and the ENJL models, fail to reproduce the shape of the experimental curve already at rather low values of Q^2.

2.2 *More on the CχQM*

Concerning the failure of the matching between long and short distances in models of large-N_c QCD, I would like to point out that there is, however, a class of low-energy observables, governed by integrals of specific QCD Green's functions, for which the CχQM predictions encoded in the MG–Lagrangian, in spite of its limitations, can be rather reliable. This is the case when the leading short-distance behaviour of the underlying Green's functions of a given observable is governed by perturbative QCD. Interesting examples of this class of observables are the decay rate $\pi^0 \to e^+e^-$, the hadronic vacuum polarization and the hadronic light-by-light scattering contributions to a low-energy observable like the anomalous magnetic moment of the muon: $\frac{1}{2}(g_\mu - 2)$. Furthermore, as recently pointed out by Weinberg [22], the MG–Lagrangian in the large-N_c limit, modulo the addition of a finite number of local counterterms [23], is a renormalizable Lagrangian. Calculations with the MG–Lagrangian, compared to those with the more sophisticated approaches described above, have the advantage of simplicity and, when applied to this class of low-energy observables, can provide a check to the more elaborated phenomenological approaches. The fact that one is dealing with a renormalizable quantum field theory is, of course, a welcome feature.

The CχQM effective Lagrangian in question is the following:

$$\begin{aligned}\mathcal{L}_{\mathrm{C}\chi\mathrm{QM}}(x)=&\underbrace{i\,\bar{Q}\gamma^{\mu}\left(\partial_{\mu}+\Gamma_{\mu}+iG_{\mu}\right)Q-\frac{i}{2}g_{\mathrm{A}}\,\bar{Q}\gamma^{\mu}\gamma_5\xi_{\mu}Q-M_Q\bar{Q}Q}_{M-G}\\&-\frac{1}{2}\bar{Q}\left(\Sigma-\gamma_5\Delta\right)Q\\&+\underbrace{\frac{1}{4}{F_{\pi}}^2\mathrm{tr}[D_{\mu}UD^{\mu}U^{\dagger}_{M-G}}+U^{\dagger}\chi+\chi^{\dagger}U]\\&-\underbrace{\frac{1}{4}\sum_{a=1}^{8}G^{(a)}_{\mu\nu}G^{(a)\mu\nu}}_{M-G}+e^2C\;\mathrm{tr}(Q_{\mathrm{R}}\mathrm{U}Q_{\mathrm{L}}U^{\dagger})\\&+L_5\;\mathrm{tr}D_{\mu}U^{\dagger}D^{\mu}U(\chi^{\dagger}U+U^{\dagger}\chi)\\&+L_8\;\mathrm{tr}(U\chi^{\dagger}U\chi^{\dagger}+U^{\dagger}\chi U^{\dagger}\chi)\,.\end{aligned}\tag{2.4}$$

The underbraced terms are those of the MG–Lagrangian, but in the presence of external $SU(3)$ vector $v_{\mu}(x)$ and axial-vector $a_{\mu}(x)$ sources. The field matrix $U(x)$ is the same 3×3 unitary matrix in flavour space which collects the Goldstone fields as in eq. (1.1). The vector field matrix $D_{\mu}U$ is also the same covariant derivative of U as in eq. (1.1) with respect to the same external sources:

$$D_{\mu}U=\partial_{\mu}U-ir_{\mu}U+iUl_{\mu},\qquad l_{\mu}=v_{\mu}-a_{\mu},\qquad r_{\mu}=v_{\mu}+a_{\mu},\tag{2.5}$$

and, with $U=\xi\xi$,

$$\begin{aligned}\Gamma_{\mu}&=\frac{1}{2}[\xi^{\dagger}(\partial_{\mu}-ir_{\mu})\xi+\xi(\partial_{\mu}-il_{\mu})\xi^{\dagger}],\\\xi_{\mu}&=i[\xi^{\dagger}(\partial_{\mu}-ir_{\mu})\xi-\xi(\partial_{\mu}-il_{\mu})\xi^{\dagger}].\end{aligned}\tag{2.6}$$

The gluon field matrix in the fundamental representation of colour $SU(3)$ is $G_{\mu}(x)$ and $G^{(a)}_{\mu\nu}(x)$ is its corresponding gluon field strength tensor. The presence of external scalar $s(x)$ and pseudoscalar $p(x)$ sources induces extra terms proportional to

$$\chi=2B[s(x)+ip(x)]\,,\tag{2.7}$$

where B, like F_{π}, is an order parameter which has to be fixed from experiment. When these sources are frozen to the up, down, and strange light quark masses of the QCD Lagrangian,

$$\chi=2B\mathcal{M},\quad\text{with}\quad\mathcal{M}=\mathrm{diag}(m_u,m_d,m_s),\tag{2.8}$$

and then

$$\Sigma=\xi^{\dagger}\mathcal{M}\xi^{\dagger}+\xi\mathcal{M}^{\dagger}\xi,\qquad\Delta=\xi^{\dagger}\mathcal{M}\xi^{\dagger}-\xi\mathcal{M}^{\dagger}\xi.\tag{2.9}$$

With the axial coupling fixed to $g_{\mathrm{A}}=1$, the extra couplings L_5 and L_8 are the only terms which are needed to absorb the ultraviolet (UV) divergences when the constituent

quark fields $Q(x)$ are integrated out (we disregard divergent couplings involving external fields alone to lowest order in the chiral expansion). If one wants to consider the case where photons are also integrated out then, to leading order in the chiral expansion and in the electric charge coupling e, the last term in the second line is also required to absorb further UV divergences. Loops involving pion fields are subleading in the $1/N_c$ expansion and hence, following the observation of Weinberg [22], the Lagrangian in eq. (2.4), when considered within the framework of the large-N_c limit, is a renormalizable Lagrangian.

3. General properties of large-N_c QCD

An interesting feature of large-N_c QCD which I shall discuss next is the fact that two-point functions of colour singlet composite local operators become simple harmonic sums in this limit.

In full generality (for a clear introduction to the appropriate mathematics literature, see e.g. ref. [32]), a harmonic sum is characterized by a base function (in our case the kernel in the dispersion relation which the two-point function in question obeys) and a Dirichlet series.

$$\Sigma(s) = \sum_{n=1}^{\infty} \lambda_n \mu_n^{-s}, \tag{3.1}$$

where μ_n are called the frequencies (the position of the narrow states in the Minkowski region in our case) and λ_n the amplitudes (the residues of the corresponding poles).

The simplest example of a Dirichlet series is the Riemann zeta function:

$$\zeta(s) = \sum_{n=1}^{\infty} n^{-s} = \prod_{\text{primes}(p)} \frac{1}{1-(1/p^s)}, \qquad \text{Re}(s) > 1, \tag{3.2}$$

where $\lambda_n = 1$ and $\mu_n = n$. The Euler product expression in the RHS extends to all prime numbers p.

3.1 *The* $\Pi_{\text{LR}}(Q^2)$ *self-energy as a harmonic sum*

Let us consider again the left–right correlation function in the chiral limit as an example to illustrate these properties. In the large-N_c limit, the spectral function $\frac{1}{\pi}\text{Im}\Pi_{\text{LR}}(t)$ is the sum of an infinite number of narrow states

$$\frac{1}{\pi}\text{Im}\Pi_{\text{LR}}(t) = -F_\pi^2 \delta(t) + \sum_{n=1}^{\infty} (-1)^{n+1} F_n^2 \delta(t - M_n^2) \tag{3.3}$$

with positive weights for the vector-like components and negative weights for the axial-vector-like components. The first term is the contribution from the pion pole. Inserting this spectral function in the dispersion relation in eq. (2.3) we find

$$-\frac{Q^2}{F_\pi^2}\Pi_{\text{LR}}(Q^2) = 1 - \sum_{n=1}^{\infty} (-1)^{n+1} \frac{F_n^2}{F_\pi^2} \frac{1}{1+(M_n^2/Q^2)}. \tag{3.4}$$

This is a typical harmonic sum which we can write as follows:

$$1 + \frac{Q^2}{F_\pi^2}\Pi_{\rm LR}(Q^2) = \sum_{n=1}^{\infty} \lambda_n \; B_{\rm LR}\left(\mu_n \frac{M_\rho^2}{Q^2}\right), \tag{3.5}$$

where ($M_\rho \equiv M_1$)

$$\lambda_n = (-1)^{n+1}\frac{F_n^2}{F_\pi^2} \quad \text{and} \quad \mu_n = \frac{M_n^2}{M_\rho^2} \tag{3.6}$$

and where the base function is

$$B_{\rm LR}(x) = \frac{1}{1+x}\,. \tag{3.7}$$

The crucial property of harmonic sums is that they have a factorizable Mellin transform (the Mellin transform of a function $F(z)$: $\mathcal{M}[F(z)](s)$ is defined by the integral $\mathcal{M}[F(z)](s) = \int_0^\infty {\rm d}z z^{s-1}F(z)$, in the domain of s where the integral exists and elsewhere by its analytic continuation). In our case

$$\mathcal{M}\left[1 + \frac{Q^2}{F_\pi^2}\Pi_{\rm LR}(Q^2)\right](s) = \mathcal{M}[B_{\rm LR}(x)](s)\Sigma(s), \tag{3.8}$$

with

$$\mathcal{M}[B_{\rm LR}(x)](s) = \Gamma(s)\Gamma(1-s), \tag{3.9}$$

and $\Sigma(s)$ the Dirichlet series in eq. (3.1) with λ_n and μ_n defined in eq. (3.6). Inverting the Mellin transform in eq. (3.8) results then in the following Mellin–Barnes representation:

$$-\frac{Q^2}{F_\pi^2}\Pi_{\rm LR}(Q^2) = 1 - \frac{1}{2\pi i}\int_{c-i\infty}^{c+i\infty} {\rm d}s \; \left(\frac{M_\rho^2}{Q^2}\right)^{-s} \Sigma(s)\Gamma(s)\Gamma(1-s), \tag{3.10}$$

where the integration path lies in the so-called fundamental strip [32] which is defined by the intersection of the convergence domain of the base function (${\rm Re}(s) \in]0,+1[$ in our case), with the domain of absolute convergence of the Dirichlet series $\Sigma(s)$. Notice that in full generality, independently of the large-N_c approximation, $\Pi_{\rm LR}(Q^2)$ also has a Mellin–Barnes representation like the one in eq. (3.10), except that then $\Sigma(s)$ is the Mellin transform of the spectral function $\frac{1}{\pi}{\rm Im}\tilde{\Pi}_{\rm LR}(t)$ where the tilde means that the contribution from the pion pole has been removed:

$$\Sigma(s) = \frac{M_\rho^2}{F_\pi^2}\int_0^\infty \frac{{\rm d}t}{M_\rho^2}\left(\frac{t}{M_\rho^2}\right)^{-s}\frac{1}{\pi}\,{\rm Im}\tilde{\Pi}_{\rm LR}(t). \tag{3.11}$$

This integral, in the large-N_c limit, becomes the Dirichlet series:

$$\begin{aligned}\Sigma(s) \;&=\; \int_0^\infty \frac{{\rm d}t}{F_\pi^2}\left(\frac{t}{M_\rho^2}\right)^{-s}\frac{1}{\pi}{\rm Im}\tilde{\Pi}_{\rm LR}(t)\\ &\underset{\text{Large-}N_c}{\Rightarrow} \sum_{n=1}^{\infty}(-1)^{n+1}\frac{F_n^2}{F_\pi^2}\left(\frac{M_n^2}{M_\rho^2}\right)^{-s}.\end{aligned} \tag{3.12}$$

The Mellin–Barnes representation is very useful. All the dynamics is encoded in the factorized Dirichlet series $\Sigma(s)$ or, in full generality, in the Mellin transform of the spectral function. The dependence in Q^2 is completely factorized from the details of the spectrum, and one can read off the asymptotic behaviours for small Q^2 (i.e. the chiral expansion) and large-Q^2 (i.e. the short-distance expansion or OPE expansion) in a straightforward way (applications of this property of the Mellin–Barnes representation in QED and QCD have been recently discussed in refs [33–35] and references therein). These asymptotic behaviours can be obtained from the so-called inverse mapping theorem [32] as follows:

- The coefficients $\mathsf{a}_{\mathsf{p},k}$ of the singular series expansions at the left of the fundamental strip, i.e.

$$\Sigma(s)\Gamma(s)\Gamma(1-s) \asymp \sum_{\Re\mathsf{p}\geq 0} \sum_{k=0}^{N(\mathsf{p})} \frac{\mathsf{a}_{\mathsf{p},k}}{(s+\mathsf{p})^{k+1}} \tag{3.13}$$

  govern the asymptotic expansion:

$$-\frac{Q^2}{F_\pi^2}\Pi_{\mathrm{LR}}(Q^2) \underset{Q^2\to\infty}{\sim} 1 - \sum_{\Re\mathsf{p}\geq 0} \sum_{k=0}^{N(\mathsf{p})} \frac{(-1)^k}{k!}\, \mathsf{a}_{\mathsf{p},k} \left(\frac{M_\rho^2}{Q^2}\right)^{\mathsf{p}} \log^k \frac{M_\rho^2}{Q^2}\,. \tag{3.14}$$

- The coefficients $\mathsf{b}_{\mathsf{p},k}$ of the singular series expansions at the right of the fundamental strip, i.e.

$$\Sigma(s)\Gamma(s)\Gamma(1-s) \asymp \sum_{\Re\mathsf{p}\geq 1} \sum_{k=0}^{N(\mathsf{p})} \frac{\mathsf{b}_{\mathsf{b}_{\mathsf{p},k}}}{(s-\mathsf{p})^{k+1}} \tag{3.15}$$

  govern the asymptotic expansion:

$$-\frac{Q^2}{F_\pi^2}\Pi_{\mathrm{LR}}(Q^2) \underset{Q^2\to 0}{\sim} 1 - \frac{(-1)^{k+1}}{k!} \sum_{\Re\mathsf{p}\geq 1} \sum_{k=0}^{N(\mathsf{p})} \mathsf{b}_{\mathsf{p},k} \left(\frac{M_\rho^2}{Q^2}\right)^{-\mathsf{p}} \log^k \frac{M_\rho^2}{Q^2}\,. \tag{3.16}$$

The sum structure over the poles p in the RHS of these equations is completely general for any two-point function. When applied to the left–right correlation function there are, however, further specific restrictions to take into account:

- The fact that in the OPE of $\Pi_{\mathrm{LR}}(Q^2)$ there are no operators of dimension two and four implies that

$$\mathsf{a}_{0,0} = 1 \qquad \text{and} \qquad \mathsf{a}_{1,0} = 0, \tag{3.17}$$

  and hence

$$\Sigma(0) = 1 \qquad \text{and} \qquad \Sigma(-1) = 0. \tag{3.18}$$

  This is precisely the content of the Weinberg sum rules, conventionally written as follows:

$$\int_0^\infty \frac{\mathrm{d}t}{F_\pi^2}\frac{1}{\pi}\mathrm{Im}\tilde{\Pi}_{\mathrm{LR}}(t) = 1, \quad \text{1st Weinberg sum rule} \tag{3.19}$$

and

$$\int_0^\infty \frac{\mathrm{d}t}{F_\pi^2}\frac{t}{M_\rho^2}\frac{1}{\pi}\mathrm{Im}\tilde{\Pi}_{\mathrm{LR}}(t) = 0, \quad \text{2nd Weinberg sum rule.} \tag{3.20}$$

Notice, however, that in full generality sum rules like

$$\Sigma(s) = \int_0^\infty \frac{\mathrm{d}t}{F_\pi^2}\left(\frac{t}{M_\rho^2}\right)^{-s}\frac{1}{\pi}\mathrm{Im}\tilde{\Pi}_{\mathrm{LR}}(t) = 0, \tag{3.21}$$

at the left of the fundamental strip where $s \leq 0$, have to be understood as analytic continuations of the Mellin transform of the spectral function (or the Dirichlet series in the large-N_c approximation) in the region of s of absolute convergence. It is in this sense that the two Weinberg sum rules should be understood.

- Because of the absolute convergence of $\Sigma(s)$ at the right of the fundamental strip, all the poles in the corresponding series expansion must be simple poles, hence $N(\mathsf{p}) = 0$ in eq. (3.16), which means that the expansion at small Q^2 is a pure power series.

4. Toy models of large-N_c QCD

As we have seen, the phenomenological applications of large-N_c QCD we have discussed in §2, rely on the limitation of the hadronic spectrum to a finite number of narrow states. In order to test this approximation and in the absence of a solution of QCD in the large-N_c limit, one has to resort to models to investigate the issue (early work on models of this type can be found in refs [36–38] and references therein). As we shall see, some of these models bring in functions of analytic number theory with quite interesting features.

4.1 *The Hurwitz model* $\Pi_{\mathrm{LR}}(Q^2)$

This is a model where the spectral function of the left–right correlation function consists of an infinite number of narrow states

$$\begin{aligned}\frac{1}{\pi}\mathrm{Im}\Pi_{\mathrm{LR}}(t) \;=\; & -F_\pi^2\delta(t) + F_{\mathrm{V}}^2\sum_{n=0}^{\infty}\delta(t - M_{\mathrm{V}}^2 - n\sigma^2) \\ & -F_{\mathrm{A}}^2\sum_{n=0}^{\infty}\delta(t - M_{\mathrm{A}}^2 - n\sigma^2)\,,\end{aligned} \tag{4.1}$$

with the vector states and the axial-vector states equally spaced by an amount σ. Implementing the two Weinberg sum rules in this spectral function reduces the number of independent parameters to F_π, the lowest vector mass M_{V} and the value of $g_{\mathrm{A}} = M_{\mathrm{V}}^2/M_{\mathrm{A}}^2$, with M_{A} the lowest axial-vector states. The other parameters are then fixed as follows:

$$F_{\mathrm{V}}^2 = F_{\mathrm{A}}^2 = F_\pi^2\,\frac{1+g_{\mathrm{A}}}{1-g_{\mathrm{A}}}\,, \quad \sigma^2 = M_{\mathrm{V}}^2\left(1+\frac{1}{g_{\mathrm{A}}}\right) \quad \text{and} \quad g_{\mathrm{A}} = \frac{M_{\mathrm{V}}^2}{M_{\mathrm{A}}^2}\,. \tag{4.2}$$

Notice that this forces the inequality

$$g_{\mathrm{A}} < 1 \quad \text{and therefore} \quad M_{\mathrm{A}}^2 > M_{\mathrm{V}}^2\,. \tag{4.3}$$

The Mellin–Barnes representation in this model is then:

$$-\frac{Q^2}{F_0^2}\Pi_{\rm LR}(Q^2) = 1 - \frac{g_{\rm A}}{1-g_{\rm A}}\,\frac{1}{2\pi i}\int_{c-i\infty}^{c+i\infty} {\rm d}s\,\left(1+\frac{1}{g_{\rm A}}\right)^{1-s} \times\left\{\zeta\left(s,\frac{g_{\rm A}}{1+g_{\rm A}}\right)-\zeta\left(s,\frac{1}{1+g_{\rm A}}\right)\right\} \times\left(\frac{M_{\rm V}^2}{Q^2}\right)^{-s}\Gamma(s)\Gamma(1-s)\,, \tag{4.4}$$

where $\zeta(s,v)$ is the Hurwitz function, a generalization of the Riemann zeta function, defined by the series:

$$\zeta(s,v)=\sum_{n=0}^{\infty}\frac{1}{(n+v)^s}\,,\quad \text{Re}\,s>1\,,\ \text{with}\ v\ \text{a fixed real number}\quad 0<v\leq 1\,, \tag{4.5}$$

and its analytic continuation. For $v=1$ it reduces to the Riemann zeta function.

The Hurwitz function is a special case of the so-called Dirichlet L-functions [39]. It has an integral representation in terms of a Mellin transform:

$$\Gamma(s)\zeta(s,v)=\int_0^{\infty}{\rm d}x\;x^{s-1}\frac{{\rm e}^{-vx}}{1-{\rm e}^{-x}}\,,\quad \text{Re}\,s>0, \tag{4.6}$$

which sets the basis for its analytic continuation [39]. The so defined $\zeta(s,v)$ is analytic for all s except for a simple pole at $s=1$ with residue 1.

Comparing eq. (4.4) with eq. (3.10), we see that the relevant Mellin transform of the Hurwitz model is

$$\Sigma_{\rm HM}(s)=\frac{g_{\rm A}}{1-g_{\rm A}}\left(1+\frac{1}{g_{\rm A}}\right)^{1-s}\left[\zeta\left(s,\frac{g_{\rm A}}{1+g_{\rm A}}\right)-\zeta\left(s,\frac{1}{1+g_{\rm A}}\right)\right]. \tag{4.7}$$

A plot of this Mellin transform is shown in figure 3. Notice the zeros at $s=-1,-3,\ldots$. These zeros are in fact quite generic of the model and they occur at odd negative values of s. The origin of it is due to the property that, for $s=-m$ with $m=0,1,2,\ldots$:

$$\zeta(-m,v)=-\frac{B_{m+1}(v)}{m+1}\,, \tag{4.8}$$

where $B_{m+1}(v)$ denotes the Bernoulli polynomial of degree $m+1$. This fact plus the symmetry property

$$B_m(1-x)=(-1)^m B_m(x)\,, \tag{4.9}$$

is at the origin of the zeros of the Mellin transform at $s=-1,-3,-5,\ldots$. Notice also that the values of the Mellin transform at negative even integer values $s=-2,-4,-6,\ldots$ are fixed by the values of Bernoulli polynomials ($m=0,1,2,3,\ldots$):

$$\Sigma_{\rm HM}(-2m)=\frac{F_0^2}{M_{\rm V}^2}\frac{g_{\rm A}}{1-g_{\rm A}}\left(1+\frac{1}{g_{\rm A}}\right)^{1+m} \times\frac{1+(-1)^m}{m+1}B_{m+1}\left(\frac{1}{1+g_{\rm A}}\right). \tag{4.10}$$

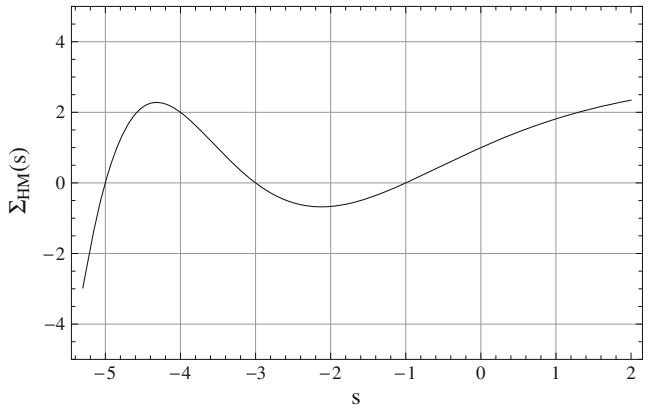

Figure 3. Plot of the Mellin transform of the Hurwitz model in eq. (4.7) for $g_A = 1/2$.

At this stage, it is interesting to compare the Mellin transform of the Hurwitz model with the one of the MHA approximation discussed in §2. This is shown in figure 4. What emerges from this comparison is that the two Mellin transforms do not differ much in the region $-1.5 \lesssim s \lesssim 1.5$, the reason being that they both satisfy the two Weinberg sum rules. The pion mass difference was rather well reproduced with the MHA approximation in eq. (2.2) because this observable is governed by the slope of the Mellin transform at $s = -1$:

$$\frac{\mathrm{d}}{\mathrm{d}s}\Sigma(s)\bigg|_{s=-1} = -\int_0^\infty \frac{\mathrm{d}t}{F_\pi^2}\frac{t}{M_V^2}\log\left(\frac{t}{M_V^2}\right)\frac{1}{\pi}\mathrm{Im}\tilde{\Pi}_{LR}(t). \tag{4.11}$$

The two Mellin transforms in figure 4 have, however, very different behaviours outside the interval $-1.5 \lesssim s \lesssim 1.5$; not so much for positive s-values (corresponding to the

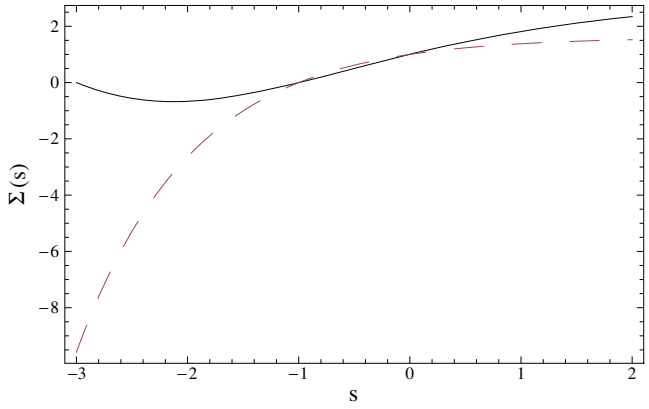

Figure 4. Mellin transforms of the Hurwitz model (solid curve) and MHA (dashed curve).

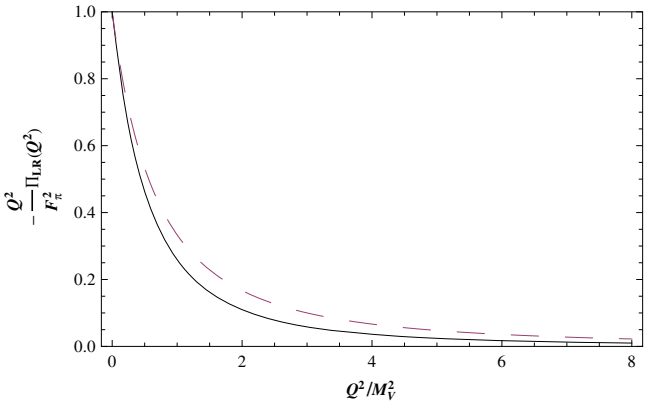

Figure 5. $-(Q^2/M_V^2)\Pi_{LR}(Q^2)$ for the Hurwitz model (solid curve) and MHA (dashed curve).

chiral expansion), but they differ quite dramatically for negative s-values (corresponding to the OPE expansion) where one finds: ($z = Q^2/M_V^2$):

$$-\frac{Q^2}{F_\pi^2}\Pi_{LR}(Q^2)\Big|_{MHA} \underset{z\to\infty}{\sim} \frac{2}{z^2} - \frac{6}{z^3} + \frac{14}{z^4} - \frac{30}{z^5} + \frac{62}{z^6} + \mathcal{O}\left(\frac{1}{z^7}\right), \qquad (4.12)$$

while

$$-\frac{Q^2}{F_\pi^2}\Pi_{LR}(Q^2)\Big|_{HM} \underset{z\to\infty}{\sim} \frac{2}{3z^2} - \frac{2}{z^4} + \frac{14}{z^6} + \mathcal{O}\left(\frac{1}{z^8}\right). \qquad (4.13)$$

We can see that, except for the first term, the signs are different and the discrepancy in magnitude increases for each successive term. Yet, the shapes of the two correlation functions in the Euclidean, as seen in figure 5, are not so different.

From these considerations we conclude that it is the Mellin transform of the spectral function (and its analytic continuation) which encodes all the details of the underlying dynamics. One can also see that the determination of higher-order condensates, the equivalent of the coefficients in the high-Q^2 expansion in eqs (4.12) and (4.13), is very sensitive to the nature of the hadronic spectrum. This is an important issue for phenomenology because, for example, the coefficient of $\mathcal{O}(1/Q^6)$ in the expansion of $\Pi_{LR}(Q^2)$ plays a crucial role in our understanding of direct CP-violation in K-decays, the so-called ϵ'/ϵ contribution [40]. Unfortunately, this $\mathcal{O}(1/Q^6)$ term, as well as the higher-order ones, appear to be very sensitive to the underlying dynamics. It is not surprising that the phenomenological determinations of these coefficients found in the literature (see e.g. refs [41,42] and references therein) differ so much.

5. The Riemann zeros and sum rules

In the previous section we have considered a model from analytic number theory to illustrate some physical features of large-N_c QCD which we would like to understand. Here I shall do the contrary, I shall consider the physical framework of dispersion relations in quantum field theory to discuss a well-known problem in Mathematics. The problem has

to do with the positions of the zeros of the Riemann zeta function defined by eq. (3.2) and its analytic continuation (for a nice elementary treatment of the Riemann zeta function, see e.g. refs [43,44]) which extends to all values of s except at $s = 1$ where it has a simple pole with residue 1.

The interesting object for our purpose is the logarithmic derivative of the Riemann zeta function which, using the Euler product expression in eq. (3.2), can be written as a Dirichlet series:

$$-\frac{\zeta'(s)}{\zeta(s)} = \sum_{\text{primes } p} \log(p) \sum_{k=1}^{\infty} p^{-ks}$$

$$= \underbrace{\sum_{n=1}^{\infty} \Lambda(n) n^{-s}}_{\text{Dirichlet series}}, \quad \text{Re}(s) > 1, \tag{5.1}$$

where $\Lambda(n)$ (n integer) are the so-called Von Mangoldt amplitudes:

$$\Lambda(n) = \begin{cases} \log(p), & \text{if } n = p^k \\ 0, & \text{otherwise} \end{cases}. \tag{5.2}$$

A plot of the Von Mangoldt amplitudes for the first hundred integers is shown in figure 6.

In fact, there exists an explicit expression for the analytic continuation of the Dirichlet series in eq. (5.1), which follows from Hadamard's product formula for $\zeta(s)$ [44]:

$$\Sigma_{\text{VonM}}(s) \equiv -\frac{\zeta'(s)}{\zeta(s)} = \log\frac{1}{2\pi} + \frac{s}{s-1}$$

$$+ \sum_{n=1}^{\infty} \frac{s}{2n(s+2n)} - \sum_{\rho} \frac{s}{\rho(s-\rho)}. \tag{5.3}$$

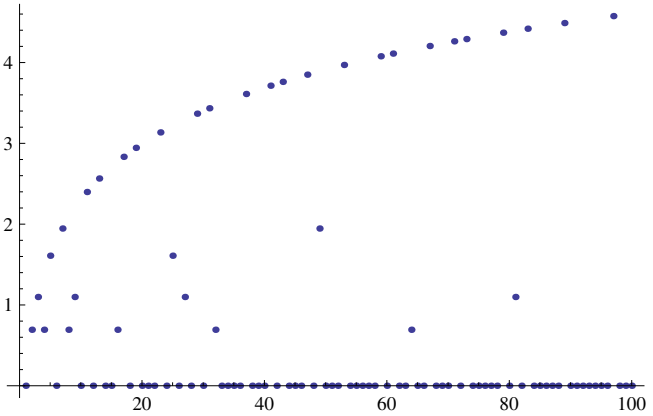

Figure 6. The Von Mangoldt values $\Lambda(n)$ for the first 100 integers. The upper curve corresponds to integer values coinciding with a prime number. The background points correspond to integers which are more than a power of a prime number. They appear as successive horizontal points.

The poles at $s = -2, -4 - 6 \cdots$ correspond to the trivial zeros of $\zeta(s)$ and the poles at $s = \rho$ to all the remaining zeros. The non-trivial zeros satisfy $0 < \mathrm{Re}(\rho) < 1$, and because of the symmetry relation $s \to 1 - s$, they must be located symmetrically relative to the vertical line $\mathrm{Re}(s) = 1/2$, the so-called critical line. The famous Riemann hypothesis (RH) states that all the non-trivial zeros have $\mathrm{Re}(s) = 1/2$. Numerically, all the non-trivial zeros which have been evaluated so far do indeed satisfy the RH.

5.1 *Question*

What are the properties of a large-N_c QCD-like Green's function which has as a spectral function the one associated to the Von Mangoldt–Dirichlet series, i.e.,

$$\frac{1}{\pi}\mathrm{Im}\Pi_{\mathrm{VonM}}(t) = \sum_{n=1}^{\infty} \Lambda(n) n M^2 \delta(t - nM^2), \tag{5.4}$$

with the amplitudes $\Lambda(n)$ given in eq. (5.2) and plotted in figure 6?

I wish to clarify the meaning of this question. From the point of view of QCD, this spectral function can only be considered, at best, as a toy model of large-N_c (perhaps as a toy model of duality violations). What seems interesting to me, however, is the fact that such an abstract mathematical question as the RH can be phrased, as we shall see next, in terms of the language familiar to physicists working in quantum field theory.

Let us call $\Pi_{\mathrm{VonM}}(q^2)$ the two-point function which has as an imaginary part called the Von Mangoldt spectral function in eq. (5.4). The function $\Pi_{\mathrm{VonM}}(q^2)$ then obeys a dispersion relation modulo subtractions. The fact that the Van Mangoldt–Dirichlet series in eq. (5.1) is defined for $\mathrm{Re}(s) > 1$ fixes the number of the required subtractions. They can be removed by taking two derivatives in the dispersion relation. This defines a function $\mathcal{P}_{\mathrm{VonM}}(z)$ in the Euclidean ($z = M^2/Q^2$), which is the analog of eq. (2.3):

$$\begin{aligned}\mathcal{P}_{\mathrm{VonM}}(z) \equiv \frac{\partial^2}{(\partial Q^2)^2}\Pi_{\mathrm{VonM}}(Q^2) &= 2\int_0^\infty \mathrm{d}t\, \frac{Q^4}{(t+Q^2)^3}\, \frac{1}{\pi}\mathrm{Im}\Pi_{\mathrm{VonM}}(t) \\ &= 2\sum_{n=1}^{\infty} \Lambda(n) \frac{nz}{(1+nz)^3},\end{aligned} \tag{5.5}$$

with the corresponding Mellin–Barnes representation ($c = \mathrm{Re}(s) \in]+1, +2[$)

$$\mathcal{P}_{\mathrm{VonM}}(z) = \frac{1}{2\pi i}\int_{c-i\infty}^{c+i\infty} \mathrm{d}s\; z^{-s}\, \Sigma_{\mathrm{VonM}}(s)\, \Gamma(s+1)\Gamma(2-s), \tag{5.6}$$

where $\Sigma_{\mathrm{VonM}}(s)$ is given in eq. (5.3). Everything is explicitly known in this representation and we can now apply the inverse mapping theorem of ref. [32] to compute the asymptotic behaviour of $\mathcal{P}_{\mathrm{VonM}}(z)$.

The interesting expansion is the short-distance expansion corresponding to large Q^2 (small-z). This expansion is governed by the singularities at the left of the fundamental strip, i.e. $s \leq 1$. The singularities at $s = -1, -2, -3, \ldots$ generated by the $\Gamma(s+1)$ factor in the integrand and by the poles in $\Sigma_{\mathrm{VonM}}(s)$ at $s = -2, -4, -6, \ldots$ corresponding to the trivial zeros of $\zeta(s)$ give rise to odd powers of

$$\mathcal{O}\left(\frac{M^2}{Q^2}\right)^{2n+1}, \qquad n = 0, 1, 2, 3, \ldots, \tag{5.7}$$

as well as to even powers ($n = 1, 2, 3, \ldots$) of

$$\mathcal{O}\left(\frac{M^2}{Q^2}\right)^{2n} \log\frac{Q^2}{M^2} \qquad \text{and} \qquad \mathcal{O}\left(\frac{M^2}{Q^2}\right)^{2n}. \tag{5.8}$$

These terms are rather analogous to the usual power terms which originate in the OPE in quantum field theory. The leading singularity at $s = 1$ gives rise to the leading asymptotic behaviour

$$\frac{1}{s-1} \Rightarrow \Gamma(2)\Gamma(1)z^{-1} = \frac{Q^2}{M^2}, \tag{5.9}$$

for Q^2 large, which is in fact rather similar to the leading behaviour of a QCD-like two-point function generated by a scalar current.

The interesting terms are of course the ones generated by the next-to-leading singularities at $s = \rho$ in the $\Sigma_{\text{VonM}}(s)$ function, i.e. the ones induced by the non-trivial zeros of the Riemann zeta function. They give rise to non-power terms:

$$-\frac{1}{s-\rho} \Rightarrow -\Gamma(\rho+1)\Gamma(2-\rho)z^{-\rho}, \tag{5.10}$$

which appear in pairs of $\mathcal{O}(Q^2/M^2)^{|\rho|}$ and $\mathcal{O}(Q^2/M^2)^{1-|\rho|}$, modulated by an oscillating behaviour in Q^2. In the particular case where $\rho = 1/2 \pm i\eta$, i.e. for the zeros satisfying the RH, these terms collapse to a unique non-power behaviour of $\mathcal{O}(\sqrt{Q^2/M^2}\,)$:

$$\begin{aligned}&\frac{-1}{s-\left(\frac{1}{2}+i\eta\right)} + \frac{-1}{s-\left(\frac{1}{2}-i\eta\right)}\\ &\quad\Rightarrow -\sqrt{\frac{Q^2}{M^2}}\,\frac{1+4\eta^2}{2}\,\frac{\pi}{\cosh\pi\eta}\cos\left(\eta\log\frac{M^2}{Q^2}\right),\end{aligned} \tag{5.11}$$

modulated by oscillating $\cos(\eta\log(M^2/Q^2))$ factors, one for each value of η along the critical line of zeros, with amplitude $(1+4\eta^2/2)(\pi/\cosh\pi\eta)$ which decay exponentially for η large.

Conclusion

The Riemann hypothesis is equivalent to the existence of a unique type of non-power terms of $\mathcal{O}(\sqrt{Q^2/M^2})$ in the short-distance expansion of the two-point function associated to the Von Mangoldt spectral function in eq. (5.4).

5.2 *Quantum mechanics sum rules*

It is perhaps helpful to discuss the previous considerations within a more general statistical mechanics framework. The discussion applies to Hamiltonians $\mathcal{H}$ with no explicit time dependence.

The probability transition amplitude in quantum mechanics is defined as

$$\langle q_f, t_f | q_i, t_i\rangle = \langle q_f | \mathrm{e}^{-i\mathcal{H}(t_f - t_i)} | q_i\rangle. \tag{5.12}$$

The evolution in imaginary time leads to a statistical mechanics interpretation which is characterized by the partition function

$$\mathcal{Z} = \mathrm{Tr}\beta\mathcal{H}\,. \tag{5.13}$$

With $t_f - t_i = -i\beta$, we then have the spectral representation:

$$\langle q_f|\mathrm{e}^{-\beta\mathcal{H}}|q_i\rangle = \sum_n \mathrm{e}^{-\beta E_n} \underbrace{\langle q_f|n\rangle\langle n|q_i\rangle}_{\Psi_n(q_f)\Psi_n^*(q_i)}\,. \tag{5.14}$$

In particular, the $\lim_{\beta\to\infty}$, i.e., $T \to 0$, $[\beta = (1/kT)]$, is governed by the ground state contribution:

$$\lim_{\beta\to\infty}\langle q_f|\mathrm{e}^{-\beta\mathcal{H}}|q_i\rangle \simeq \mathrm{e}^{-\beta E_0}\Psi_0(q_i)\Psi_0^*(q_f). \tag{5.15}$$

In general

$$E_0 = \lim_{\beta\to+\infty} -\frac{1}{\beta}\log \mathrm{Tr}\,\mathrm{e}^{-\beta\mathcal{H}}\,. \tag{5.16}$$

The following quantity

$$\mathcal{M}(\beta) \equiv \langle q_f = 0|\mathrm{e}^{-\beta\mathcal{H}}|q_i = 0\rangle = \sum_n |\Psi_n(0)|^2\mathrm{e}^{-\beta E_n} \tag{5.17}$$

is of special interest to us because it provides quantum mechanics framework for the equivalent of the quantum field theory sum rules.

The relevant Hamiltonian for our purposes is one which has levels

$$E_n = nE_0, \tag{5.18}$$

and wave functions at the origin

$$|\Psi_n(0)|^2 = \Lambda(n), \tag{5.19}$$

i.e. the Von Mangoldt amplitudes defined in eq. (5.2). Inserting this ansatz in eq. (5.17), the corresponding Mellin–Barnes representation is then

$$\mathcal{M}_{\mathrm{VonM}}(\beta) = \frac{1}{2\pi i}\int_{c-i\infty}^{c+i\infty} \mathrm{d}s(\beta E_0)^{-s}\ \Sigma_{\mathrm{VonM}}(s)\ \Gamma(s), \tag{5.20}$$

with a fundamental strip defined now by the interval $c = \mathrm{Re}(s) \in]+1, \infty[$ and $\Sigma_{\mathrm{VonM}}(s)$ the same expression as in eq. (5.3). The inverse mapping theorem applied to this formula gives us the expansion at small β, i.e. the expansion at high temperature ($\beta = 1/kT$):

$$\begin{aligned}\mathcal{M}_{\mathrm{VanM}}(\beta) \underset{\beta\to 0}{\sim}\ & \frac{1}{\beta E_0} - \frac{1}{\sqrt{\beta E_0}} \\ & \times \sum_\eta \left[\Gamma(1/2 + i\eta)\mathrm{e}^{i\eta\log(\beta E_0)} + \Gamma(1/2 - i\eta)\mathrm{e}^{-i\eta\log(\beta E_0)}\right] \\ & + \log\frac{1}{4\pi} + \beta E_0\left(\log(8\pi) - \frac{1}{2} + \sum_\rho \frac{1}{\rho(1+\rho)}\right)\end{aligned}$$

$$+ \ (\beta E_0)^2 \left[\frac{1}{2} \log(\beta E_0) - \frac{5}{12} \right.$$
$$\left. - \frac{1}{2} \log(4\pi) + \frac{1}{2}\gamma_{\rm E} - \sum_{\rho} \frac{1}{\rho(2+\rho)} \right]$$
$$+ \ \mathcal{O}\left[(\beta E_0)^3\right]. \tag{5.21}$$

In this expression the leading behaviour in the first line is the one associated with the trivial singularity at $s = 1$, while the second term in the first line gives the asymptotic behaviour reflected by the non-trivial zeros located at $s = 1/2$. The Riemann hypothesis implies that these are the only possible non-power terms in the expansion. A constant term as well as odd power terms in (βE_0), with the leading one shown in the second line, are generated because of the $\Gamma(s)$ factor in eq. (5.20) with coefficients which, except for the constant term, depend on the location of the non-trivial zeros (the sum over ρ's). The trivial singularities at $s = -2n$ generate powers in $(\beta E_0)^{2n}$ (the leading one is shown in the third line) modulated by a $\log(\beta E_0)$ factor and powers of $(\beta E_0)^{2n}$. The latter are modulated by coefficients which also depend on the positions of the non-trivial zeros (the sum over ρ's).

An interesting question which I have been investigating in collaboration with Josep Tarón is: *What is the equivalent potential which produces a spectrum of discrete levels $E_n = nE_0$ with corresponding wave functions at the origin known in modulus $|\Psi_n(0)|^2 = \Lambda(n)$, i.e. the Von Mangoldt amplitudes defined in eq. (5.2)*? I hope to have an answer for Raymond's next birthday...

Acknowledgements

The author wishes to thank M Knecht, S Peris, D Greynat, J Tarón and M Gonzalez-Alonso for many useful discussions on the topics presented here.

This work has been partially supported by the EU RTN network FLAVIAnet (Contract No. MRTN-CT-2006-035482).

References

[1] G t' Hooft, *Nucl. Phys.* **B75**, 461 (1974)
[2] C Vafa and E Witten, *Nucl. Phys.* **B72**, 461 (1974)
[3] G 't Hooft, *NATO Adv. Study Inst. Ser. B Phys.* **59**, 135 (1980)
[4] S Coleman and E Witten, *Phys. Rev. Lett.* **45**, 100 (1980)
[5] C Vafa and E Witten, *Nucl. Phys.* **B234**, 173 (1984)
[6] M Knecht, *La chromodynamique quantique à basse énergie*, cours donné à la 27eme session de l'Ecole d'Eté de Gif, La Chromodynamique Quantique sous toutes ses couleurs, LPC Clermont-Ferrand, 18–22 Sept. 1995, A.-M. Lutz ed., IN2P3
[7] E Witten, *Nucl. Phys.* **B160**, 57 (1979)
[8] S Weinberg, *Physica* **A96**, 327 (1984)
[9] J Wess and B Zumino, *Phys. Lett.* **B37**, 95 (1971)
[10] E Witten, *Nucl. Phys.* **B223**, 422 (1983)
[11] J Gasser and H Leutwyler, *Nucl. Phys.* **B250**, 465 (1985)

[12] G Ecker, J Gasser, A Pich and E de Rafael, *Nucl. Phys.* **B321**, 311 (1989)
[13] T Hambye, S Peris and E de Rafael, *J. High Energy Phys.* **027**, 0305 (2003)
[14] M Knecht and E de Rafael, *Phys. Lett.* **B424**, 335 (1998)
[15] T Das, G S Guralnik, V S Mathur, F E Low and J E Young, *Phys. Rev. Lett.* **18**, 759 (1967)
[16] M Knecht, S Peris and E de Rafael, *Phys. Lett.* **B443**, 255 (1998)
[17] M A Shifman, A I Vainshtein and V I Zakharov, *Nucl. Phys.* **B147**, 385, 447 (1979)
[18] E Witten, *Phys. Rev. Lett.* **51**, 2351 (1983)
[19] J Comellas, J I Latorre and J Tarón, *Phys. Lett.* **B360**, 109 (1995)
[20] A Manohar and G Georgi, *Nucl. Phys.* **B233**, 232 (1984)
[21] D Espriu, E de Rafael and J Tarón, *Nucl. Phys.* **B345**, 22 (1990)
[22] S Weinberg, *Phys. Rev. Lett.* **105**, 261601 (2010)
[23] E de Rafael, *Phys. Lett.* **B703**, 60 (2011)
[24] Y Nambu and G Jona-Lasinio, *Phys. Rev.* **122**, 345 (1961)
[25] J Bijnens, Ch Bruno and E de Rafael, *Nucl. Phys.* **B390**, 501 (1993)
[26] G Ecker, J Gasser, H Leutwyler, A Pich and E de Rafael, *Phys. Lett.* **B321**, 425 (1989)
[27] V Cirigliano, G Ecker, H Neufeld and A Pich, *J. High Energy Phys.* **012**, 0306 (2003)
[28] E de Rafael, *Nucl. Phys. (Proc. Suppl.)* **B119**, 71 (2003)
[29] S Peris and E de Rafael, *Phys. Lett.* **B490**, 213 (2000)
[30] P Masjuan and S Peris, *J. High Energy Phys.* **0705**, 040 (2007)
[31] ALEPH Collaboration: R Barate *et al*, *Z. Phys.* **C76**, 15 (1997); *ibid*, *Eur. Phys. J.* **C4**, 409 (1998)
[32] Ph Flajolet, X Gourdon and Ph Dumas, *Theor. Comp. Sci.* **144**, 3 (1995)
[33] S Friot, D Greynat and E de Rafael, *Phys. Lett.* **B628**, 73 (2006)
[34] J-Ph Aguilar, D Greynat and E de Rafael, *Phys. Rev.* **D77**, 093010 (2008)
[35] D Greynat and S Peris, *Phys. Rev.* **D82**, 034030 (2010)
[36] B Blok, M A Shifman and D X Zhang, *Phys. Rev.* **D57**, 2691 (1998); Erratum, *ibid.* **D59**, 019901 (1999)
[37] M Golterman, S Peris, B Phily and E de Rafael, *J. High Energy Phys.* **0201**, 024 (2002)
[38] O Catà, M Golterman and S Peris, *J. High Energy Phys.* **0508**, 076 (2005)
[39] Tom M Apostol, *Introduction to analytic number theory*, Ch.12 (Springer-Verlag, 1976)
[40] J F Donoghue and E Golowich, *Phys. Lett.* **478**, 172 (2000)
[41] M Gonzalez-Alonso, A Pich and J Prades, *Phys. Rev.* **D81**, 074007 (2010)
[42] K Maltman *et al*, arXiv:1110.5562v1 [hep-ph]
[43] Julian Havil, *GAMMA, exploring Euler's constant* (Princeton University Press, 2003)
[44] Jeffrey Stopple, *A primer of analytic number theory – From Pythagoras to Riemann* (Cambridge University Press, 2003)